Physical metallurgy and magnetic behavior of Cd stabilized bcc βGd alloys

by

Jinke Tang

A Thesis Submitted to the
Graduate Faculty in Partial Fulfillment of the
Requirements for the Degree of
MASTER OF SCIENCE

Department: Materials Science and Engineering
Major: Metallurgy

Iowa State University
Ames, Iowa

1990

TABLE OF CONTENTS

I. INTRODUCTION

Most of the rare earth metals have a close packed crystal structure (fcc, hcp or dhcp) at room temperature and a bcc structure at high temperature [1]. While the physical properties, e.g., magnetic behavior, of room temperature phases of rare earth metals have been studied extensively, little is known about the properties of the high temperature bcc phase. This is because the diffusionless transformation from bcc phase to close packed phase happens so fast that it is impossible to retain the pure bcc rare earth metal at room temperature by ordinary quenching. It was first demonstrated, however, by Gibson and Carlson that the bcc phase could be retained at room temperature by alloying with Mg and subsequent water quenching in the case of yttrium [2]. Miller and Daane [3] used this method and retained the high temperature bcc phase for heavy rare earths in an attempt to confirm the existence of a bcc high temperature allotrope in pure Gd, Tb, Dy, Ho, Er, Tm and Lu. Herchenroeder, Manfrinetti and Gschneidner were successful in stabilizing bcc γLa using the same quenching method [4]. In a systematic study

carried out on La alloys [5], it was shown that only Cd is as effective as Mg in stabilizing the bcc structure.

By utilizing the experimental results stated above, room temperature or low temperature examination of the physical properties of bcc rare earth alloys is possible. And in many cases the data obtained from these alloys can be used to estimate the properties of pure bcc rare earth metals [4,6].

Herchenroeder and Gschneidner studied extensively the physical metallurgy and magnetic behavior of Mg stabilized bcc βGd and βDy [6,7]. In the case of Gd, single phase alloy could be retained in a window around the eutectoid composition from 23.6 at.%Mg to 29 at.%Mg, where the eutectoid composition is ~26 at.%Mg [8]. These bcc Gd-Mg alloys order ferromagnetically (60 - 75 K) on cooling before undergoing a Gabay-Toulouse type spin glass transition (40 - 50 K) into a mixed ferromagnetic plus spin glass state. One of their most interesting discoveries is that the metastable Gd-Mg alloys have the highest concentration of magnetic atom among the known metallic spin glasses (> 70 at.%Gd).

The purpose of this M.S. research program is to continue the investigation on bcc Gd alloys by expanding the study to Gd-Cd system. The basis of this study rests on several observations and suppositions based on extensions of these facts. (1) Cd has been proven to be an effective stabilizer (similar to Mg) of bcc phase in the case of La [5], and therefore there is a good chance that bcc Gd phase can be retained at room temperature by alloying with Cd. (2) Gd-Cd phase diagram is known [9]. (3) The eutectoid composition of bcc βGd is ~16 at.%Cd, which suggests that the best chances of obtaining metastable bcc alloys would be near this composition [6]. This composition is significantly lower than that in Gd-Mg system, where the bcc structure was retained from 23.6 at.%Mg to 29 at.%Mg. This provides a great opportunity to study metastable bcc alloys richer in Gd (> 80 at.%Gd), especially the spin glass behavior over this composition range. (4) By combining the data of both Gd-Mg and Gd-Cd systems, we can get better extrapolated information for pure bcc Gd.

II. EXPERIMENTS

A. Sample Preparation and Characterization

The high purity Gd used in this investigation was prepared at the Materials Preparation Center of the Ames laboratory. The results of chemical analysis of such Gd are listed in Table 1. Cd with a purity of 99.999 at.%Cd was purchased from Cominco Products Inc., Electronic Materials Department. Weighed amounts of Gd and Cd were sealed in a thin walled Ta tube 50 mm long and 6 mm in diameter under helium partial pressure. Each sample weighed about 3 grams. The reason for limiting the sample weight and using thin walled Ta tube is to maximize the quenching efficiency as will be discussed later. The sealed samples were melted in a vacuum induction furnace at ~1400 °C for about 20 minutes (the melting temperature of Gd is 1313 °C [1].). In order to ensure homogeneity the crucibles were inverted and samples were remelted at ~1400 °C and then cooled to room temperature.

Table 1. Chemical analysis of Gd (ppm atomic)

Impurity[a]	Concentration
H	1089
C	170
N	67
O	766
F	< 25
Na	< 2
Al	< 3
Si	2
Cl	4
K	< 4
Fe	19
Cu	3
Nb	< 6
Hf	< 2
Ta	10
W	20
Pt	7
Tb	< 3
Yb	< 2
Lu	< 1

[a]Elements not listed have an impurity level < 1 ppm.

Quenching was done as described below. The Ta crucible containing sample was sealed in a quartz tube under He partial pressure to prevent the reaction of Ta with air when heating. It was then placed in a resistance furnace and heated for a half hour at 1200 °C, which is ~100 °C above the liquidus temperature. This was to ensure that a homogeneous melted alloy was obtained. By quickly removing the quartz tube out of furnace and breaking it, the Ta crucible was dropped into an ice water/acetone bath. The small amount of sample and a thin walled crucible used helped to reach a maximum quenching speed possible by this method.

Shown in Fig. 1 is the Gd-Cd phase diagram from 0 to 60 at.%Cd [9]. The eutectoid composition of bcc βGd is ~16 at.%Cd. Work done by Herchenroeder and Gschneidner indicated that bcc βGd could be retained by quenching from the liquid state. Quenching from within βGd region was shown not to be as effective in retaining 100% βGd as quenching from liquid state [6]. Removing the quartz tube from furnace takes some time, during which time the transformation from βGd to αGd (or from βGd to CdGd, depending on exact composition) has started. Unless a much faster quenching technique, e.g., quenching into a Ga-In eutectic melt quench bath, is used, the transformation from βGd to αGd, or

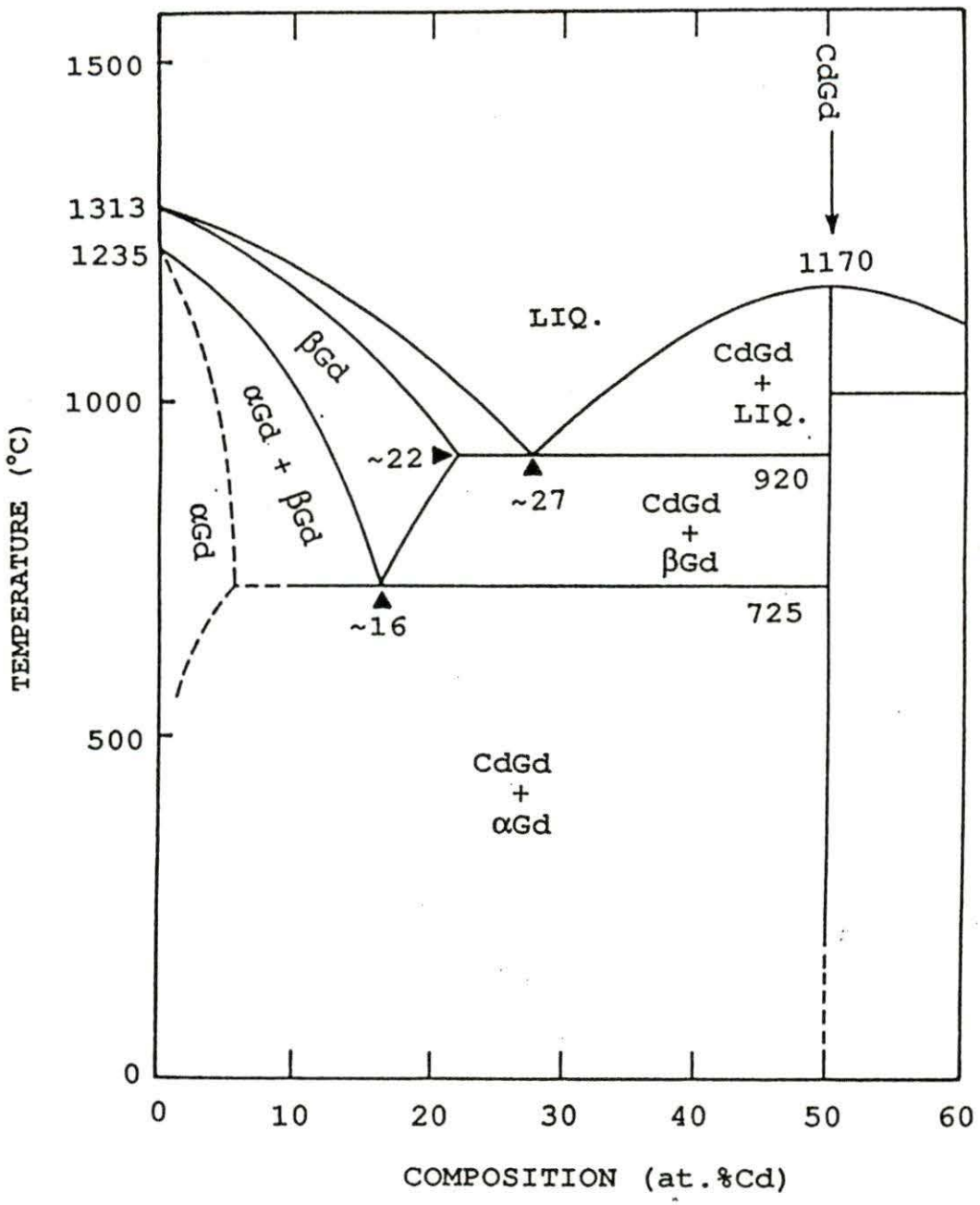

Fig. 1. The Gd-rich end of the Gd-Cd phase diagram [9]

CdGd, can not be prevented. In the case of quenching from liquid state, the time taken to remove the quartz tube out of furnace allows βGd to form first, and it is retained at room temperature because of the increased quenching rate as the cooling process continues through the temperature range encompassing the eutectoid transformation temperature.

Samples with compositions of 14, 15, 16, 17 and 19 at.%Cd were prepared by liquid quenching as described above. X-ray diffraction analyses indicated that all samples except one, 14 at.%Cd, are single phase and have the bcc structure. In the case of 14 at.%Cd, the X-ray pattern showed extra peaks from hcp αGd, which suggested that 14 at.%Cd alloy is far enough away from the eutectoid composition (16 at.%Cd) such that precipitates of αGd from bcc βGd could not be suppressed by the quenching technique used in this study.

X-ray diffraction was done on a SCINTAG diffractometer. Powder samples were not used because, as shown by Miller and Daane [3], cold working required to produce metal powder would cause the transformation from metastable bcc phase to equilibrium phases. Slices of bulk sample were mechanically polished on a

600 grit paper and on a microcloth covered lap using a fine powder suspension of Al_2O_3 in methanol. The polished samples were then etched with solution of 5 % nitric acid in water and rinsed with methanol and acetone. Samples were spun during the X-ray experiment to reduce the effect due to preferred orientation. A typical X-ray pattern obtained from a quenched bcc Gd-Cd single phase alloy is shown in Fig. 2.

Lattice parameter, $\underline{a}$, for each of these alloys were determined from X-ray data. It was noticed that, for a given alloy, the $\underline{a}$ determined from different reflection planes varied significantly and showed no systematic change, and therefore, an extrapolation method was not used to obtain $\underline{a}_o$. We believe this is due to preferred orientation in the sample, as also observed by Herchenroeder and Gschneidner [6]. $\underline{a}$ was calculated from the (211) reflection because it has a high reflection angle and a relatively high intensity. Lattice parameters so determined are listed in Table 2.

These lattice parameters were used to estimate the lattice parameter of pure bcc Gd. Shown in Fig. 3 is the $\underline{a}$ versus alloy concentration plot. A linear extrapolation to 0 %Cd gives a

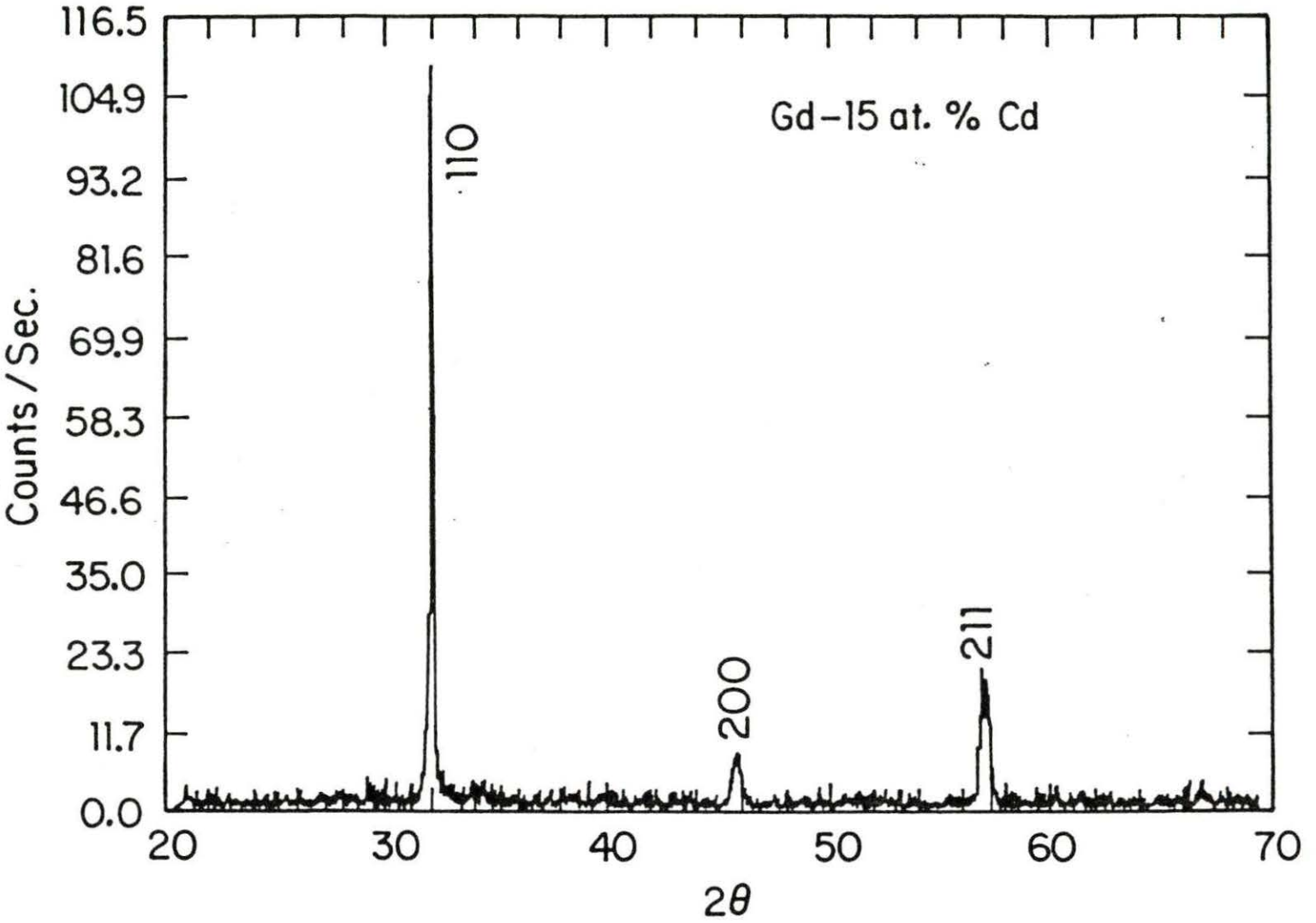

Fig. 2. X-ray diffraction pattern for quenched single phase bcc alloy Gd-15at.%Cd

Table 2. Lattice parameters of bcc Gd-Cd alloys

Alloy	$\underline{a}$ (Å)
Gd-19at.%Cd	3.944
Gd-17at.%Cd	3.944
Gd-16at.%Cd	3.942
Gd-15at.%Cd	3.957
bcc Gd (extrapolated)	3.99(4)

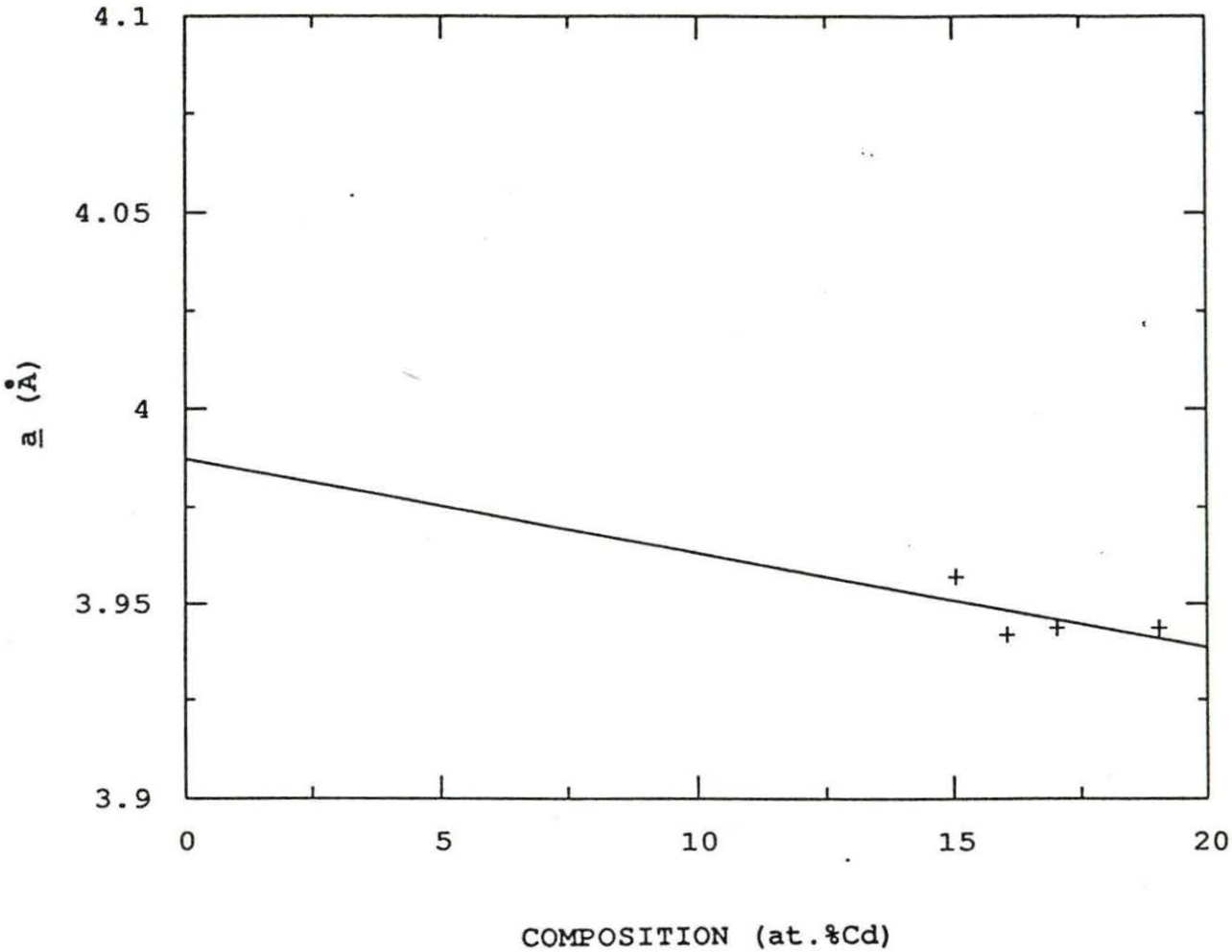

Fig. 3. Lattice parameter a versus Cd concentration of Gd-Cd alloys

lattice parameter of 3.99 ± 0.04 Å for pure bcc Gd. Compared with the values reported earlier ($\underline{a}$ = 4.06 Å, from quenched Gd-Mg bcc alloy data and $\underline{a}$ = 4.01 Å, high temperature value, corrected to room temperature [6]), one can see a reasonably good agreement between them.

Sample preparation for optical metallographic examination were carried out following a similar procedure used for preparing X-ray samples. All samples had basically the same kind of microstructure, which can be illustrated with the case of Gd-16at.%Cd, figure 4. As can be seen, it is essentially a single phase alloy. Two types of microstructure can be recognized: type 1 (as shown in the upper part of Fig. 4), where small grains of size ~5 μm form a fishnet-like pattern, and type 2 (lower part of Fig. 4) which contains rather large grains (~100 μm). Chemical analysis using EDS revealed that there is no apparent difference in Cd concentration between the two regions within the resolution of the EDS, which is about 2 at.%. However, in the type 1 region the black colored boundaries which separate small grains could be the traces of second phase. Magnetic measurements on these alloys supported this conclusion (see Sec. II, B). Since the amount of the second phase is small

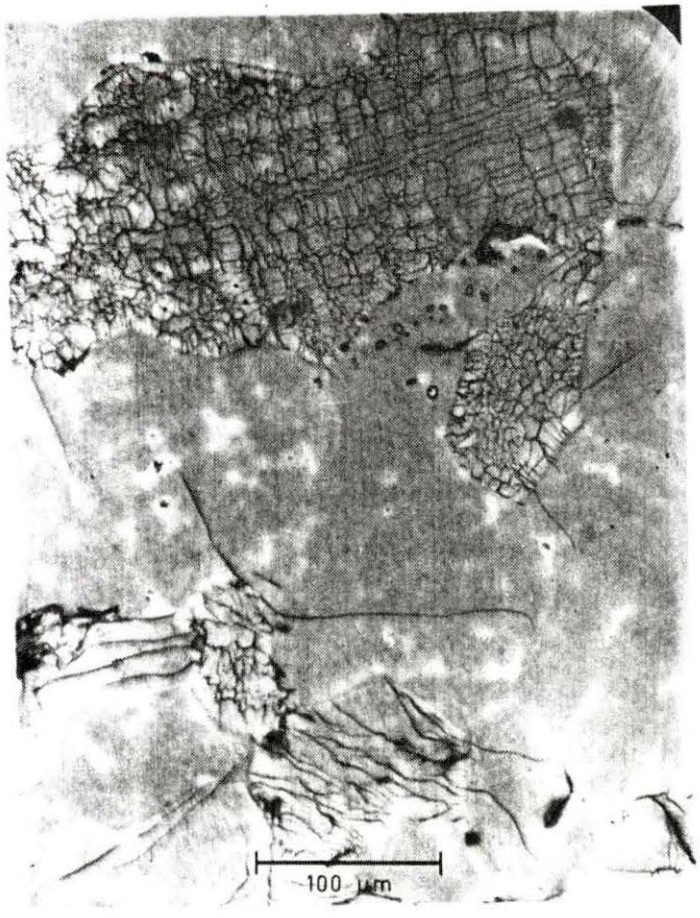

Fig. 4. Photomicrograph of Gd-16at.%Cd. Magnification: 250X

(~1 %), X-ray and EDS could not detect them. In the type 2 region, the dendritic growth from the liquid phase on quenching is evident. During quenching samples probably stayed in bcc one phase region quite long, which allowed some annealing and homogenization to take place and thus explained why the dendritic structure was somewhat smeared out.

B. Magnetic Properties

The low temperature properties of the Gd-Cd alloys were investigated by magnetic susceptibility and heat capacity measurements. Most magnetic measurements were made from 1.5 K to ~300 K using a Faraday magnetometer. A detailed description of such a magnetometer can be found in references [10] and [11]. The measuring field which varied from 0.5 T to 2 T allowed us to determine isothermal magnetization as a function of the applied field. SQUID magnetometers in Dr. Finnemore's group and Dr. McCallum's group were used to examine the low field magnetic susceptibility. Low temperature (1.3 K to 70 K) heat capacity measurements were carried out using an adiabatic heat pulse type calorimeter [11,12].

1. Magnetic susceptibility

Figure 5 shows the magnetic moment versus temperature of the Gd-17at.%Cd sample, which shows the common features of all of the Gd-Cd alloys studied. Data were taken from 1.5 K to ~300 K using different measuring fields from 0.5 T to 1.7 T. The system undergoes a ferromagnetic phase transition at ~85 K. As can be seen, the transition takes place over a quite broad temperature range. Therefore the Curie temperature T_c was determined from an Arrott plot [13]. In an Arrott plot, inverse susceptibility $1/\chi$ was plotted as a function of m^2 (m = magnetization) for a series of temperatures near T_c (Fig. 6), and then the intercepts of the $1/\chi$ versus m^2 curve with the y-axis, $(1/\chi)_{m=0}$, was plotted against the temperature (Fig. 7). T_c was determined by extrapolating the $(1/\chi)_{m=0}$ versus T plot to x-axis (Fig. 7). This procedure was repeated for all Gd-Cd alloys, and the T_c's determined for these alloys are listed in Table 3.

The fact that T_c decreases with increasing Cd concentration is not surprising. Cd addition changes the average number of Gd-Gd nearest neighbors and the average distance between them, and

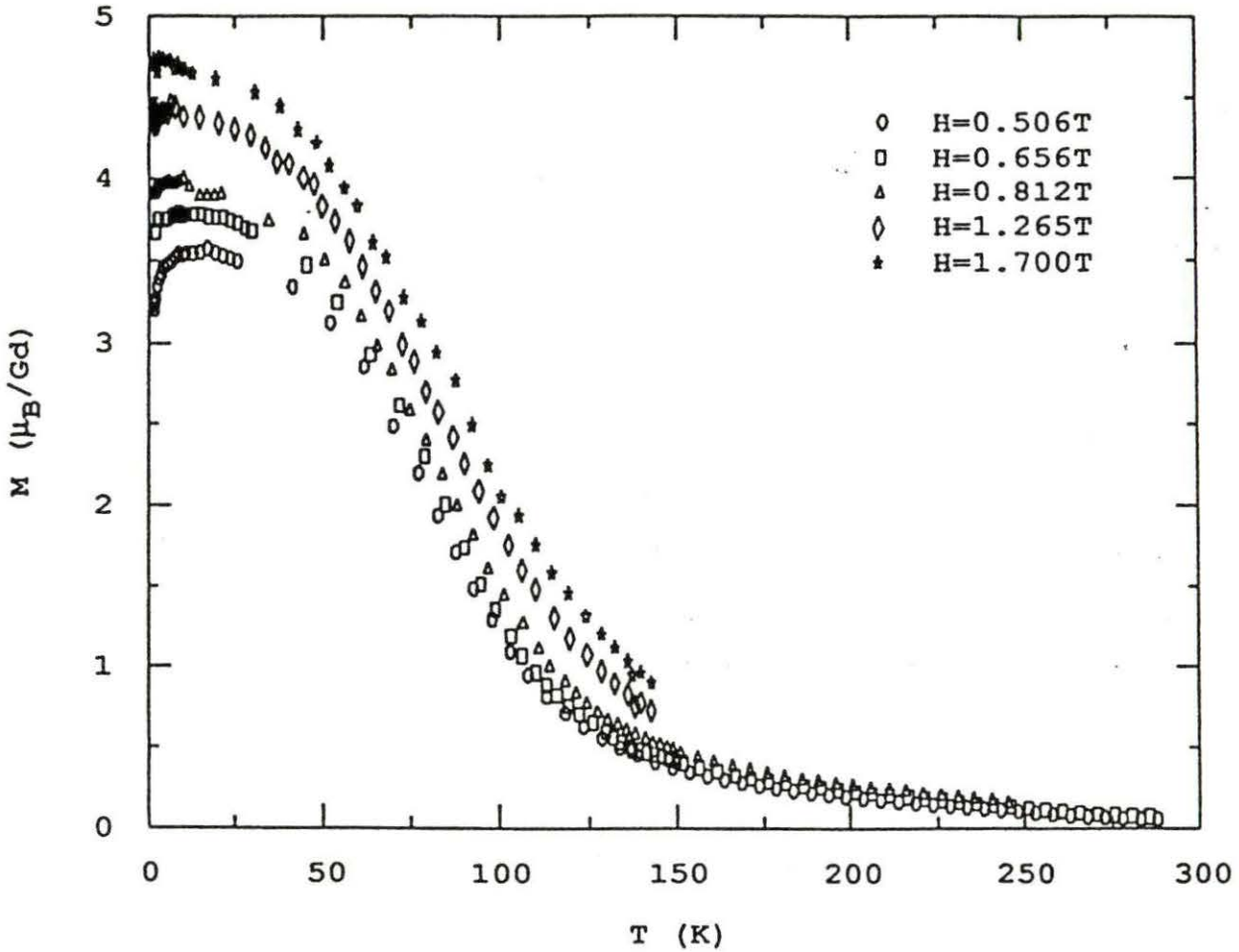

Fig. 5. Magnetic moment versus temperature for Gd-17at.%Cd. Data were taken from 1.5 K to ~300 K in fields of 0.506, 0.656 and 0.812 T and from 1.5 K to 140 K in fields of 1.265 and 1.700 T

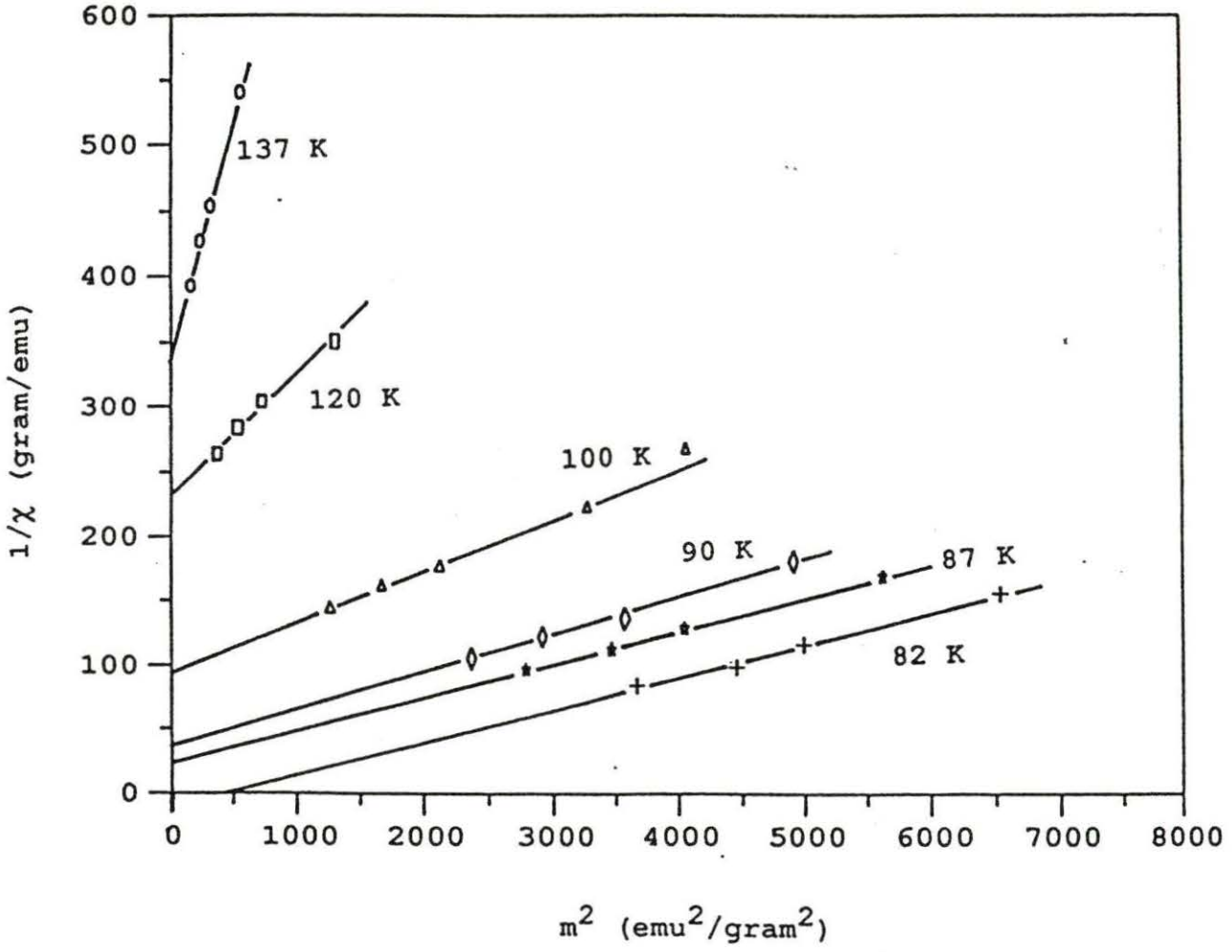

Fig. 6. Arrott plot for Gd-17at.%Cd

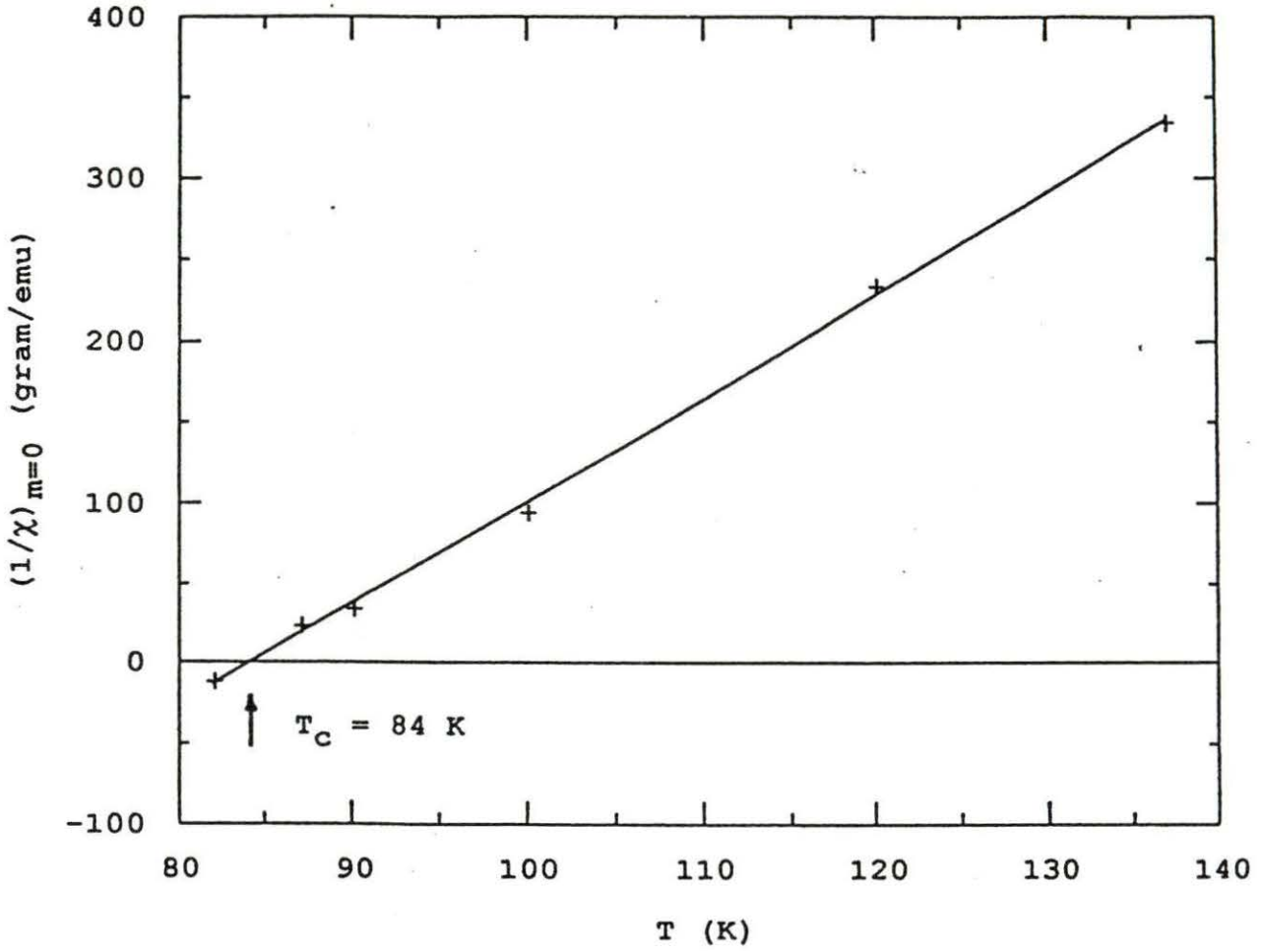

Fig. 7. $(1/\chi)_{m=0}$ versus temperature plot for Gd-17at.%Cd

Table 3. Transition temperatures of bcc Gd-Cd alloys

Alloy	T_c (K)	T_f (K)
Gd-19at.%Cd	77	36
Gd-17at.%Cd	84	25
Gd-16at.%Cd	85	23.5
Gd-15at.%Cd	88	23.5

thus weaken the strength of the RKKY interaction which is responsible for the ferromagnetic ordering in the system.

The T_C's of these alloys can be used to estimate the ordering temperature of pure bcc Gd. This was done by plotting T_C as a function of Cd concentration and extrapolating the curve to 0 %Cd (Fig. 8). The triangles in Fig. 8 are the data obtained from Gd-Cd alloys examined in this study. The data were fitted to a straight line using a least squares fit procedure. The extrapolated ordering temperature for bcc Gd is 128.5 K. The rectangles are the data from Gd-Mg system obtained by Herchenroeder and Gschneidner [7]. A similar extrapolation from a least squares fit of their data gave a T_C of 133.7 K for bcc Gd. Combining the two sets of data, one can conclude that the ordering temperature of pure bcc Gd is 131 $\pm$ 3 K. In the previous work on the Gd-Mg alloys [7], the authors estimated the T_C of bcc Gd to be 145 K. This value seems to be too high because the authors relied on the three high Mg concentration alloys and did not use a least squares fit of the data. We believe the 133.7 K value obtained from the least squares fit of their data to be more reliable.

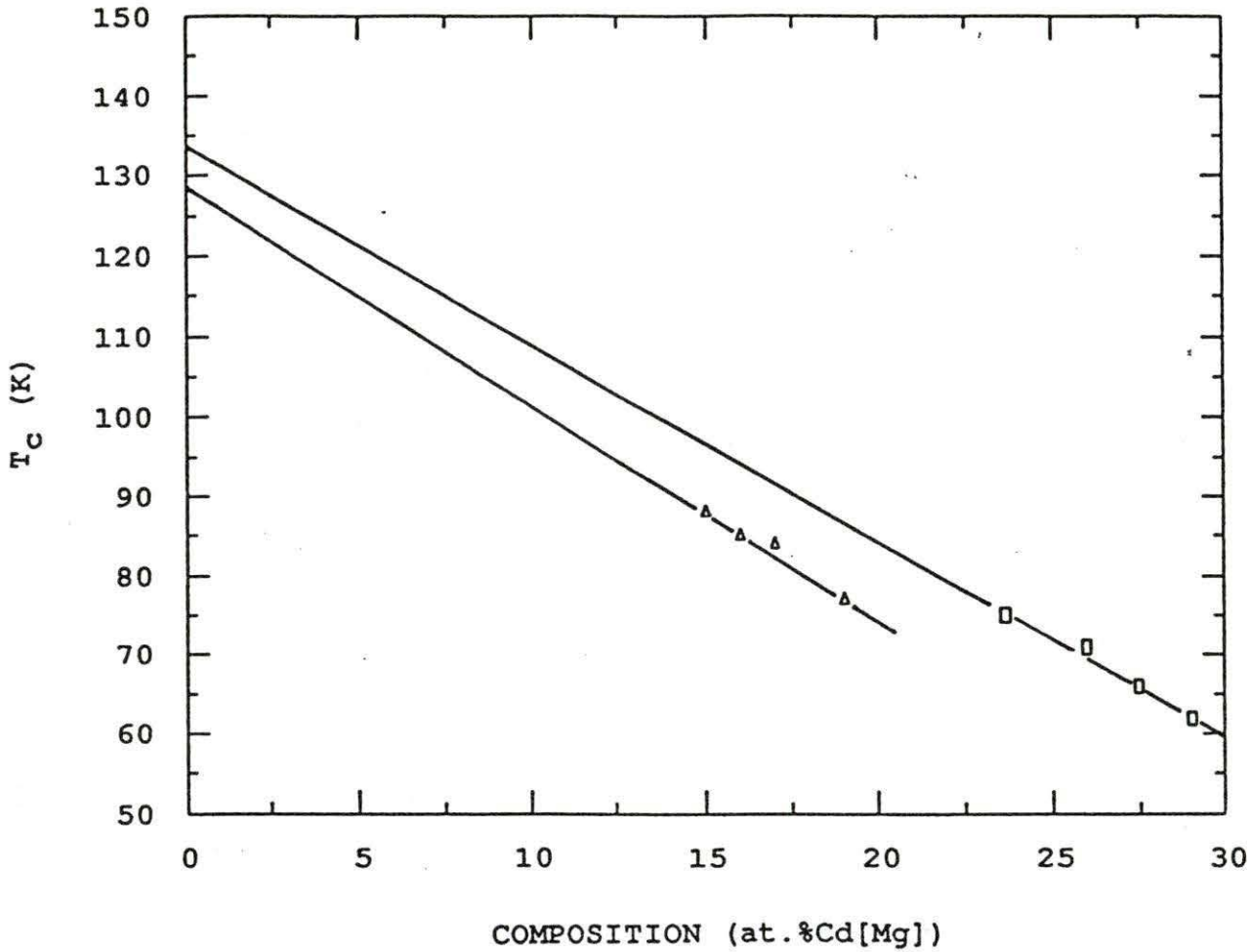

Fig. 8. The Curie temperature, T_C, as a function of Cd(Mg) concentration. The triangles are for Gd-Cd alloys and the rectangles are for Gd-Mg alloys. The lines are the least squares fit of the data

The magnetic moment associated with the ferromagnetic ordering is relatively small. Shown in Fig. 9 is the field dependence of magnetization of the Gd-17at.%Cd sample. Above T_C, the M versus H plot exhibits a straight line behavior, indicating that the system was in a paramagnetic state. Below T_C, the moment showed no sign of saturation even in a field of 1.7 T and at a temperature of 4.2 K. The maximum measured moment per Gd atom is less then 5 μ_B, which is far from the expected value of Gd, 7 μ_B [14]. This is due to the coexistence of a strong antiferromagnetic interactions within the ferromagnetically ordered state as will be discussed next.

Low field measurement usually is more sensitive to the nature of the magnetic structure, especially when antiferromagnetic interactions are involved. Therefore, the magnetic susceptibility of all samples were measured using an applied field of 50 Gauss. Shown in Fig. 10 is the χ versus T plot of the Gd-19at.%Cd sample. The measurements were made under both zero-field-cooled (ZFC) and field-cooled (FC) conditions.

At high temperature there is hardly any difference in χ for the ZFC and FC runs. But at low temperature (below ~50 K), there

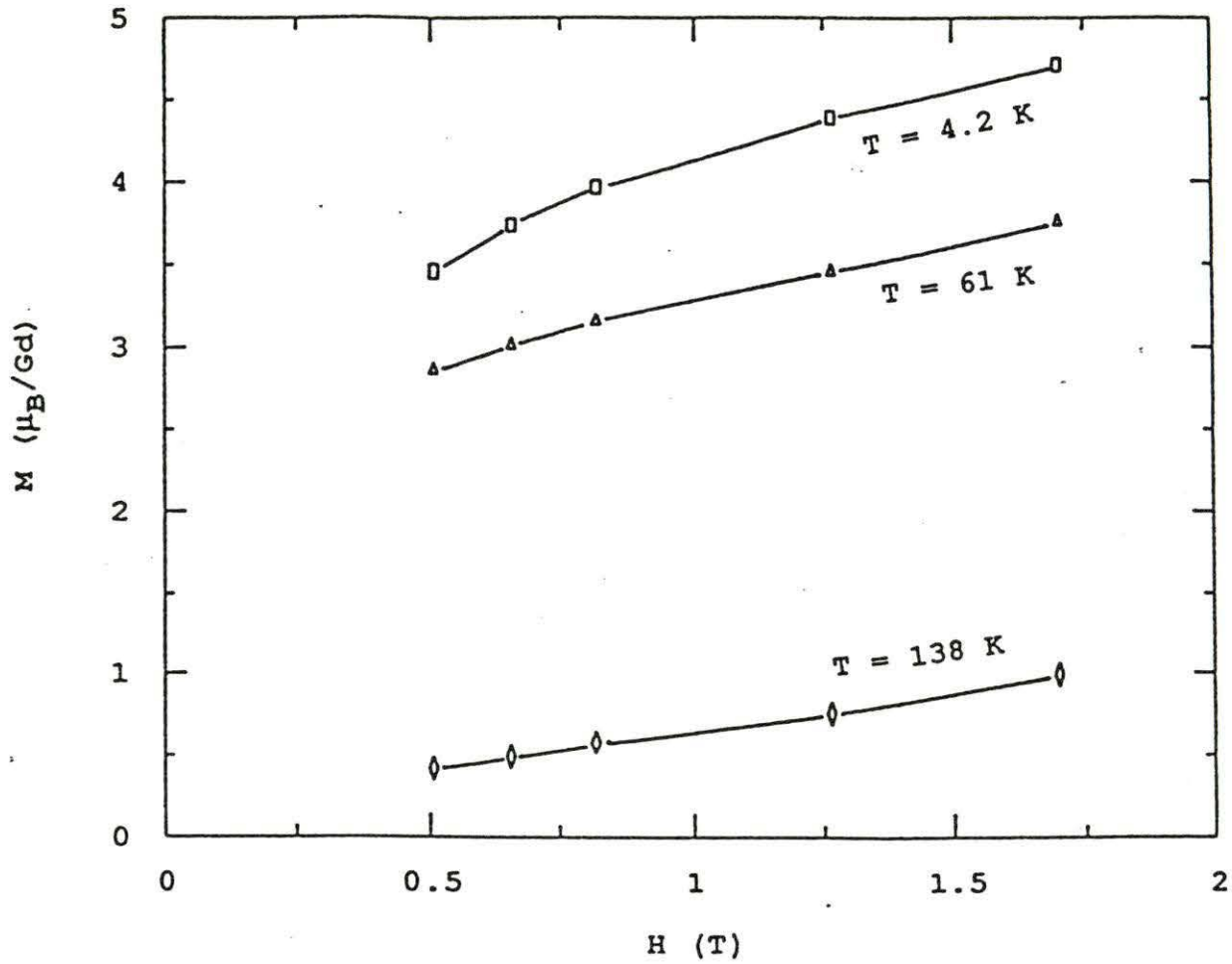

Fig. 9. Field dependence of magnetization of Gd-17at.%Cd

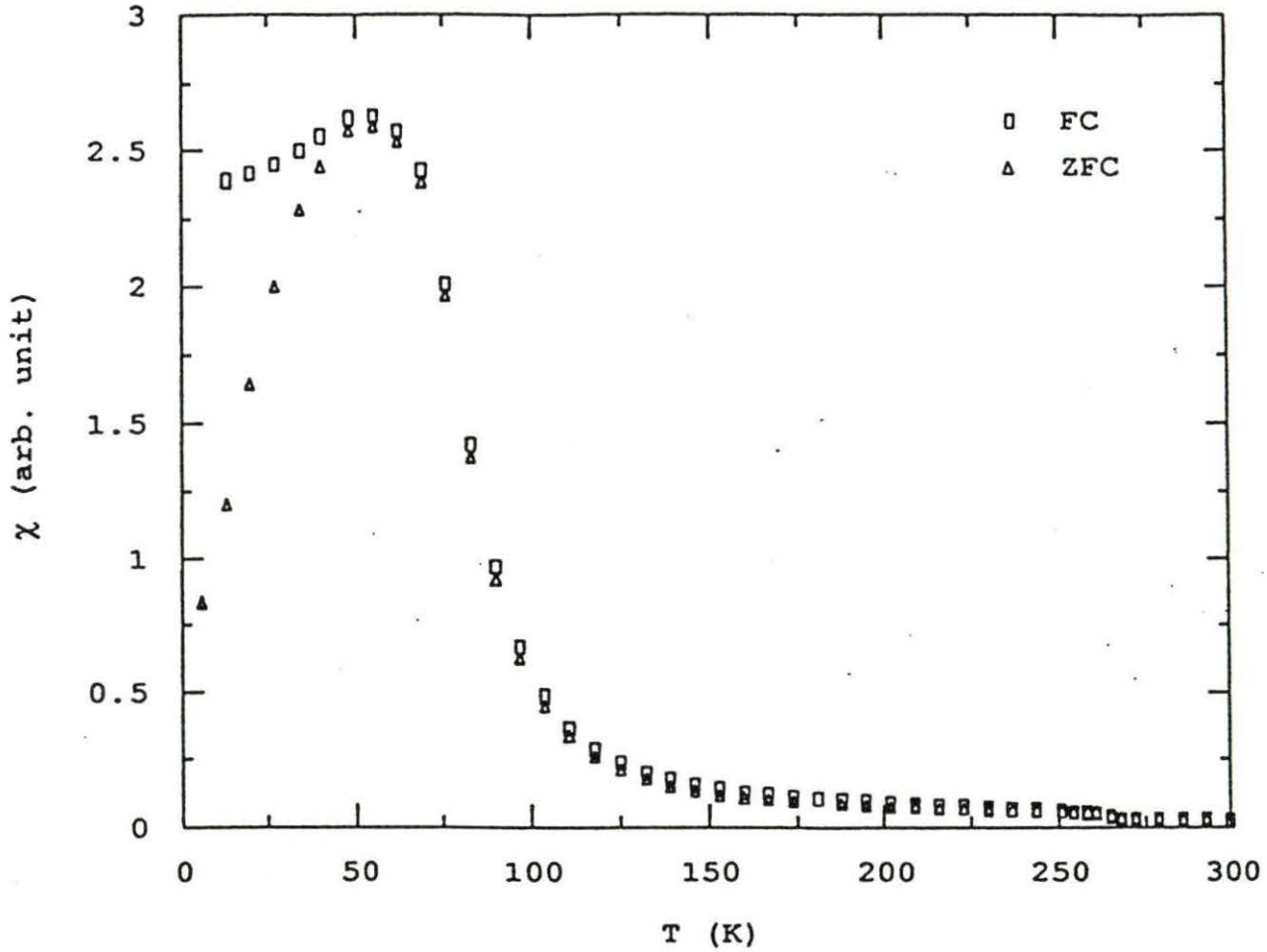

Fig. 10. Field-cooled (FC) and zero-field-cooled (ZFC) magnetic susceptibility of Gd-19at.%Cd

is a significant difference in the susceptibilities. In the ZFC case χ dropped rapidly after it reached a maximum at ~55 K; in the FC case χ is almost a constant. This is typical of spin glass behavior.

Spin glass behavior was first found in dilute metallic alloy AuFe containing ~1 at.% of magnetic impurity Fe [15]. Since the magnetic moments (of Fe) are randomly distributed throughout the lattice, the RKKY interaction between them has also the random pattern. Unlike the ferromagnetic or antiferromagnetic system, in which the RKKY interactions between the nearest neighboring spins are either positive or negative, the RKKY interaction between two spins in a spin glass system is random. This causes some spins to align parallel and some spins to align antiparallel. It is because of this competition between ferromagnetic and antiferromagnetic exchange interactions that the spins can be frustrated in trying to choose one state over another, and upon cooling the resulting state is that the spins are "frozen" in a configuration where they are oriented in random directions below a certain temperature, T_f, called the freezing temperature. When the sample is cooled in zero field, a cusp in susceptibility χ at T_f is usually found. If the sample is cooled

through T_f with the field on, a plateau in χ will be seen due to the alignment of spins by the field which are subsequently frozen in as T passes through T_f [16].

The spin glass behavior in a concentrated metallic alloy is even more interesting. As one would expect, increasing the concentration of magnetic atom leads to a conventional magnetic, ferromagnetic or antiferromagnetic, phase transition. What surprising is that, on cooling from high temperature, the system not only undergoes the paramagnetic-ferromagnetic transition, but on further cooling, it enters a spin glass state [17]. Such a ferromagnetic-spin glass transition has been studied for years. According to one of the models studied [18], as the temperature is lowered below the freezing temperature, the spin components which are transverse with respect to the applied field are frozen in due to the competition between ferromagnetic and antiferromagnetic interactions, while the colinear ferromagnetic structure remains partially intact. The low temperature phase is, therefore, characterized by the coexistence of a spontaneous magnetization (ferromagnetic order) and a spin glass ordering of the transverse components of the spins. This ferromagnetic-spin glass transition is called Gabay-Toulouse-type transition.

The ferromagnetic-spin glass transition has been observed in a number of systems such as metallic Fe_xAl_{1-x} [19], insulating $(Eu_xSr_{1-x})S$ [20] and amorphous $(Fe_xNi_{1-x})_{79}P_{13}B_8$ [21]. Recently, Herchenroeder and Gschneidner discovered that bcc Gd-Mg alloy also undergoes a ferromagnetic-spin glass transition into a mixed ferromagnetic and spin glass state [7]. These alloys are unusual in that they contain 70 - 77 at.% magnetic Gd, which is the highest concentration of magnetic atom known to exhibit spin glass behavior in a metallic system. It is of interest to find out how high the concentration can go before the spin glass behavior vanishes.

The irreversible magnetic susceptibility between ZFC and FC found in Gd-19at.%Cd (Fig. 10) is universal among the Gd-Cd alloys suggesting that all alloys undergoes a Gabay-Toulouse-type phase transition from the ferromagnetic state to the ferromagnetic + spin glass mixed state. Spin glass behavior exists over such a high concentration (81 - 85 at.%Gd) indicates the strong competition between ferromagnetic and antiferromagnetic interactions existing in the ferromagnetically ordered state.

The freezing temperature T_f was determined for all Gd-Cd alloys studied. For an ordinary spin glass transition (paramagnetic-spin glass transition), T_f is marked by a sharp cusp in χ_{ZFC}. While in the case of ferromagnetic-spin glass transition, the cusp in χ_{ZFC} is no longer seen due to the spin alignment in the ferromagnetic state. Therefore T_f is normally defined as the intersection between a linear extrapolation of the low temperature side of χ_{ZFC} and a horizontal line defined by χ_{ZFC} maximum. Such a procedure to determine T_f is illustrated in Fig. 11. The T_f's which were determined in this manner are listed in Table 3. It is clear that T_f decreases with increasing Gd composition. It implies that as the ferromagnetic coupling between Gd atoms gets stronger (as a result of increasing Gd concentration), the spin glass state becomes weaker.

The spin glass state can be gradually destroyed by an increasing applied magnetic field as shown in Fig. 5 (All measurements were done when sample was zero-field-cooled.). If, for simplicity, T_f is taken as the temperature where M versus T plot reaches a maximum, T_f is pushed down to below 17 K in a field of 0.5 T and below 9 K in a field of 0.8 T. The spin glass

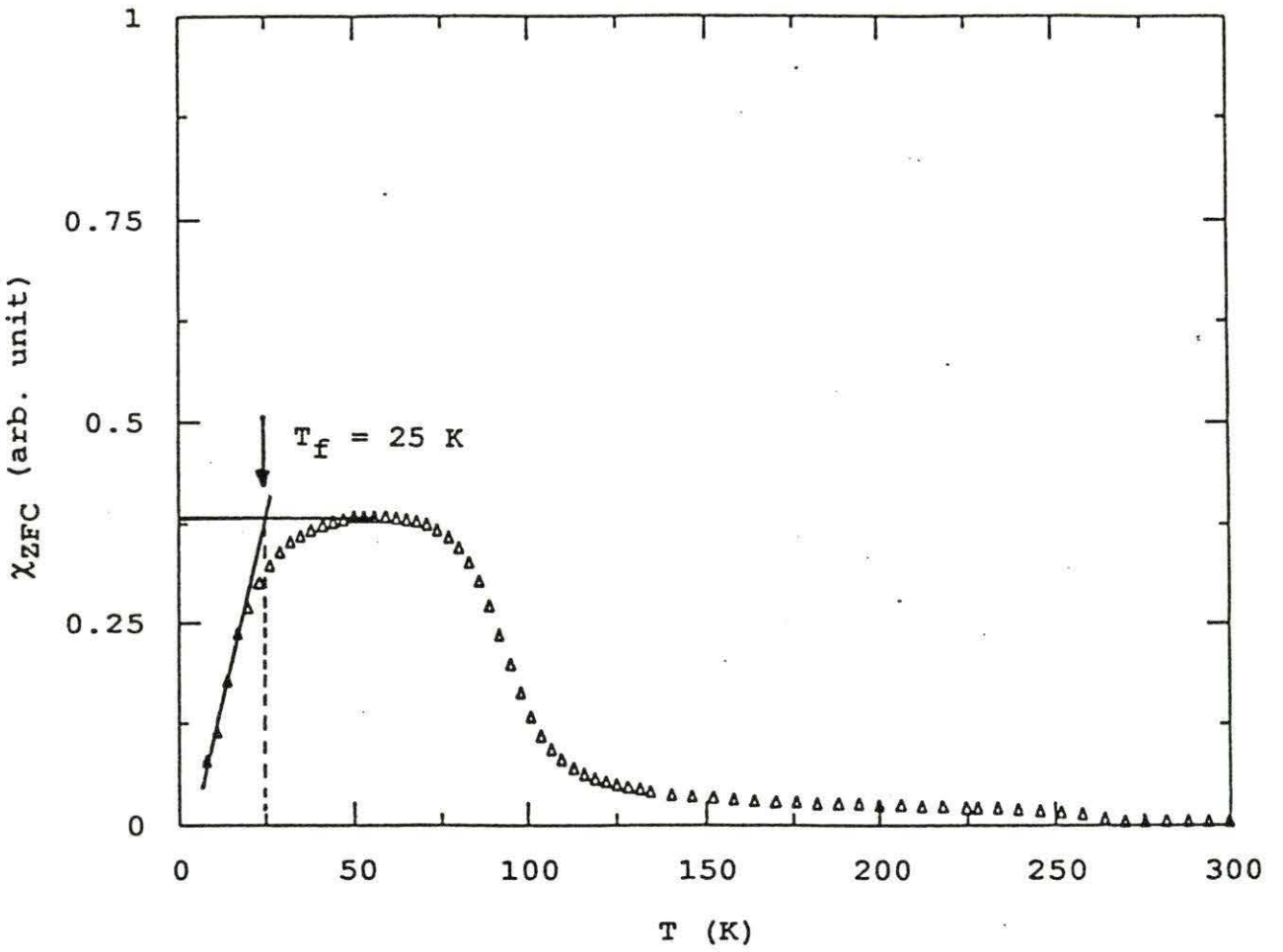

Fig. 11. The determination of spin glass freezing temperature T_f for Gd-17at.%Cd

state is completely suppressed when a field of 1.7 T is applied, and the M versus T curve looks just like that of an ordinary ferromagnet.

A detailed examination revealed a small step in low field susceptibility at ~260 K in all samples (see Fig. 10 and Fig. 11). This is probably due to the presence of a second phase in the samples. The most probably second phase would be either αGd or CdGd as discussed in Sec. A. Both of them order ferromagnetically. While αGd has a Curie temperature just below room temperature (T_C = 293 K) [14], the T_C of CdGd is reported to be 254 - 265 K [22,23], which is the temperature where the step in χ develops. Although it seems to be more likely that CdGd exists in the samples as an impurity phase because its T_C is near the step in χ, the presence of αGd in the samples is also possible. It was shown by Herchenroeder and Gschneidner [7] that the Curie temperature of the αGd-Mg alloys decreases linearly with increasing Mg concentration. The T_C reaches as low as 250 K for a concentration of 5 at.%Mg. Therefore, it is possible that the T_C in a αGd-Cd alloy of concentration of ~5 at.%Cd is in the vicinity of 250 - 260 K.

The amount of CdGd (αGd) can be estimated from a magnetization M versus applied field H plot by extrapolating the curve to zero field and finding the intercept M_0. Shown in Fig. 12 is the M versus H plot for Gd-17at.%Cd at 206 K. At such a temperature, the magnetic ordering of impurity CdGd (αGd) has already well developed, but the bulk sample is still in a paramagnetic state. Therefore, M versus H plot should have a straight line behavior and the extrapolation of the straight line to zero field, M_0, is the spontaneous magnetization of impurity CdGd (αGd). Since the saturation moment is 6 μ_B/Gd for pure CdGd [22] (7.6 μ_B/Gd for pure αGd [14]), a M_0 of 0.062 μ_B/Gd infers that less than 1 % of the total Gd atoms is in impurity phase CdGd (αGd), which is consistent with the metallographic results, see Fig. 4.

Due to the presence of the impurity phase, susceptibility χ does not follow the Curie-Weiss law at high temperatures.

2. Heat capacity

It is well known that the low temperature heat capacity, C, of an ordinary metallic material as a function of temperature can be written as

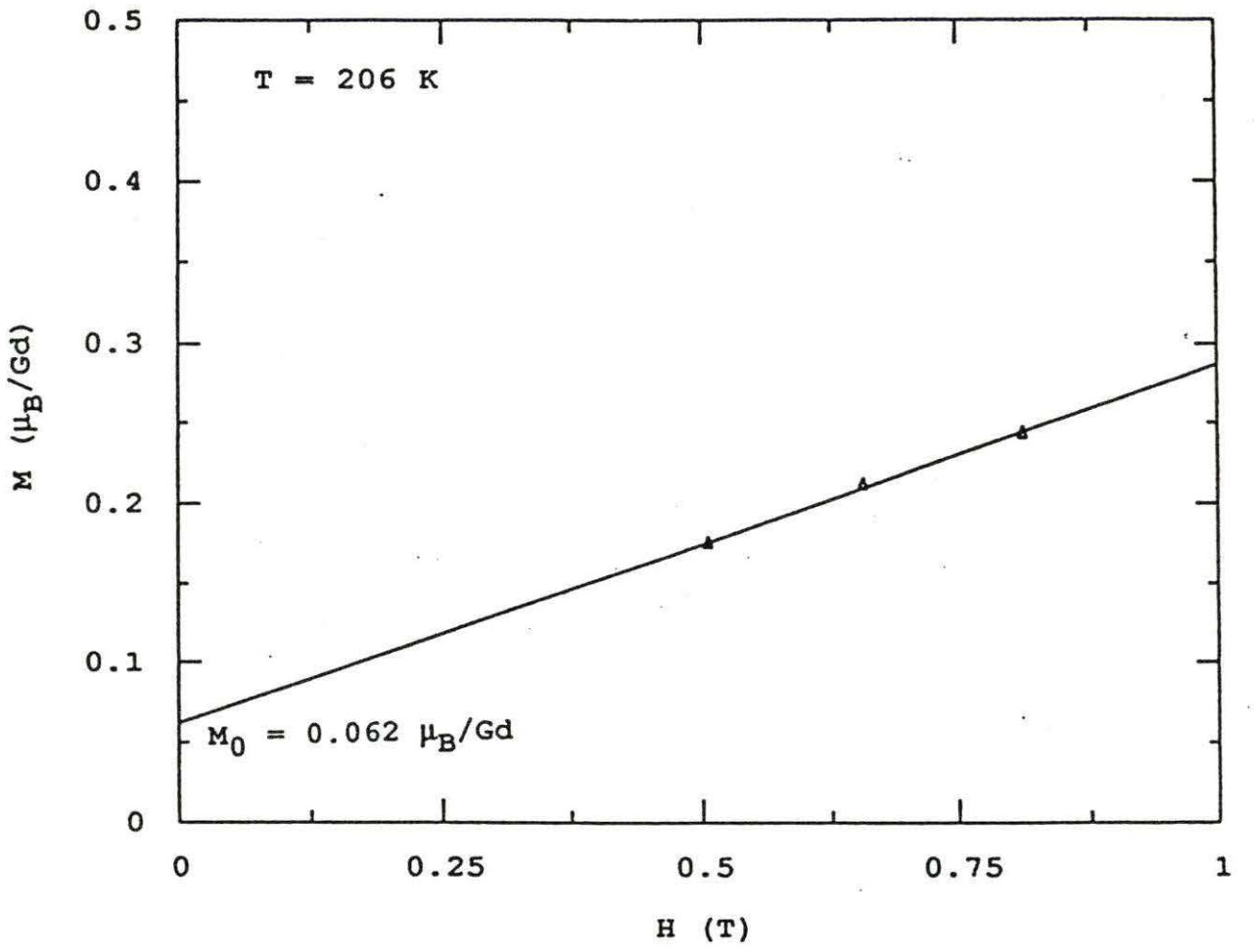

Fig. 12. Magnetization versus applied field for Gd-17at.%Cd at 206 K

$$C = \gamma T + \beta T^3. \qquad (1)$$

The linear term in Equation (1) is the electronic contribution to the heat capacity, and γ is the electronic specific heat coefficient. The cubic term is the lattice heat capacity with $\beta = 1944/\theta_D^3$ J/g.at. K^4, where θ_D is the Debye temperature of the lattice [24]. For magnetic materials, an additional term, C_m, is added to the total heat capacity. The form of C_m depends on the types of the magnetic ordering. In the case of Gd-Cd alloy system, C_m is the sum of spin glass heat capacity and ferromagnetic heat capacity because the low temperature phase is a mixed spin glass + ferromagnetic phase. The spin glass heat capacity is normally characterized by a linear term in temperature below T_f [25,26], and the ferromagnetic heat capacity has a $T^{3/2}$ behavior at low temperature [24]. Therefore, the total heat capacity can be expressed as

$$C = \gamma' T + \beta T^3 + \delta T^{3/2}, \qquad (2)$$

where γ' is the sum of the spin glass contribution and electronic contribution γ.

The heat capacity of Gd-16at.%Cd measured from 1.6 K to 40 K is shown in Fig. 13. Since Equation (2) holds only at the lowest temperatures, the experimental data were fitted over the

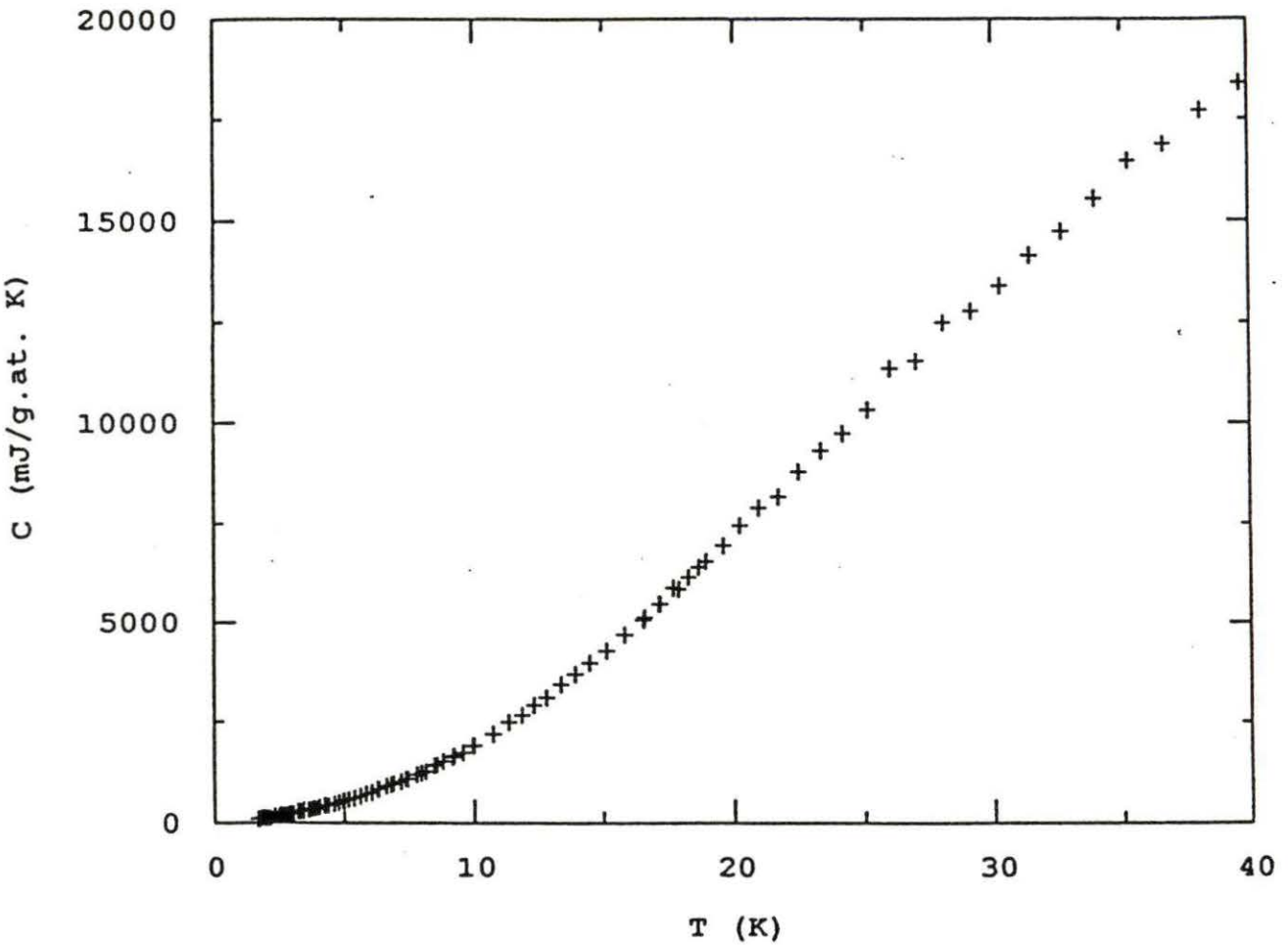

Fig. 13. Heat capacity of Gd-16at.%Cd measured from 1.6 K to 40 K

temperature range 1.6 K < T < 5 K. The fitting was done through a least squares fit method, and constants γ', β and δ were thus determined. Shown in Fig. 14 is the function $\gamma' T + \beta T^3 + \delta T^{3/2}$ obtained from the fitting (solid line) together with the experimental data (crosses). As seen, the excellent agreement between the two is obvious.

$\gamma' = 26 \pm 2$ mJ/g.at. K^2 is the sum of spin glass contribution and electronic contribution to the heat capacity. To separate the two is difficult. Leung, Wang and Harmon [27] predicted that γ for ferromagnetic bcc Gd is 11.4 mJ/g.at. K^2. If this value is taken as an estimate of the real γ of Gd-16at.%Cd, the linear coefficient of spin glass heat capacity, $\gamma' - \gamma$, is about 15 mJ/g.at. K^2.

Debye temperature θ_D was calculated from constant β ($\beta = 0.68 \pm 0.05$ mJ/g.at. K^4). A θ_D of 142 K for Gd-16at.%Cd is slightly lower than those determined for Gd-Mg system, where θ_D is about 170 - 190 K [7]. Comparing the Debye temperatures of Cd and Mg, which is 120 K and 318 K, respectively with that of αGd (169 K) [14,28], it is reasonable to believe that Cd addition would lower the θ_D of bcc Gd and Mg addition would increase θ_D.

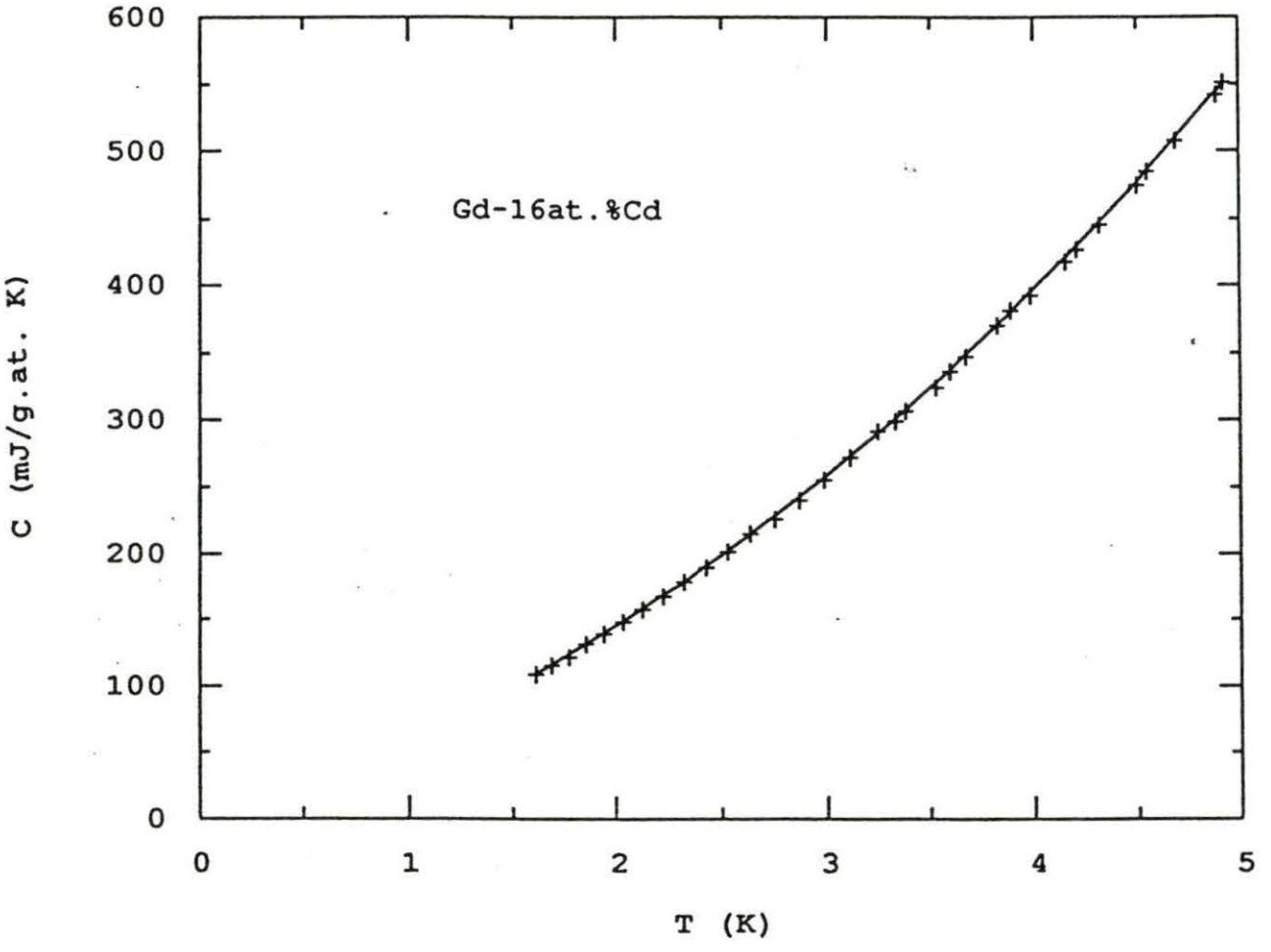

Fig. 14. Low temperature, 1.6 K < T < 5 K, heat capacity (crosses) and the least squares fit (solid line)

(Debye temperature also depends on the crystal structure in addition to the force constants between the atoms and their masses. Strictly speaking, Cd addition does not necessarily lower the θ_D of bcc Gd because of its low θ_D. But it is true the Cd and most Cd intermetallics are soft materials.) Based on the above assumption, the Debye temperature of pure bcc Gd would be expected lie somewhere between 140 K and 170 K.

δ determined from the fitting is 31 $\pm$ 1 mJ/g.at. $K^{5/2}$, which is about the same as the ones found in the Gd-Mg system [7].

The successful fitting of Equation (2) to experimental data suggests that the heat capacity can be easily separated into lattice, ferromagnetic, spin glass and electronic heat capacities. In another words, it indicates that both ferromagnetic state and spin glass state exist in the system even at the lowest temperatures, supporting the conclusion that the system is in a mixed spin glass + ferromagnetic state below T_f. Figure 15 shows a C/T versus T^2 plot for lattice heat capacity (triangles), ferromagnetic heat capacity (diamonds), sum of spin glass and electronic heat capacity (squares) and total heat capacity (circles) of sample Gd-16at.%Cd.

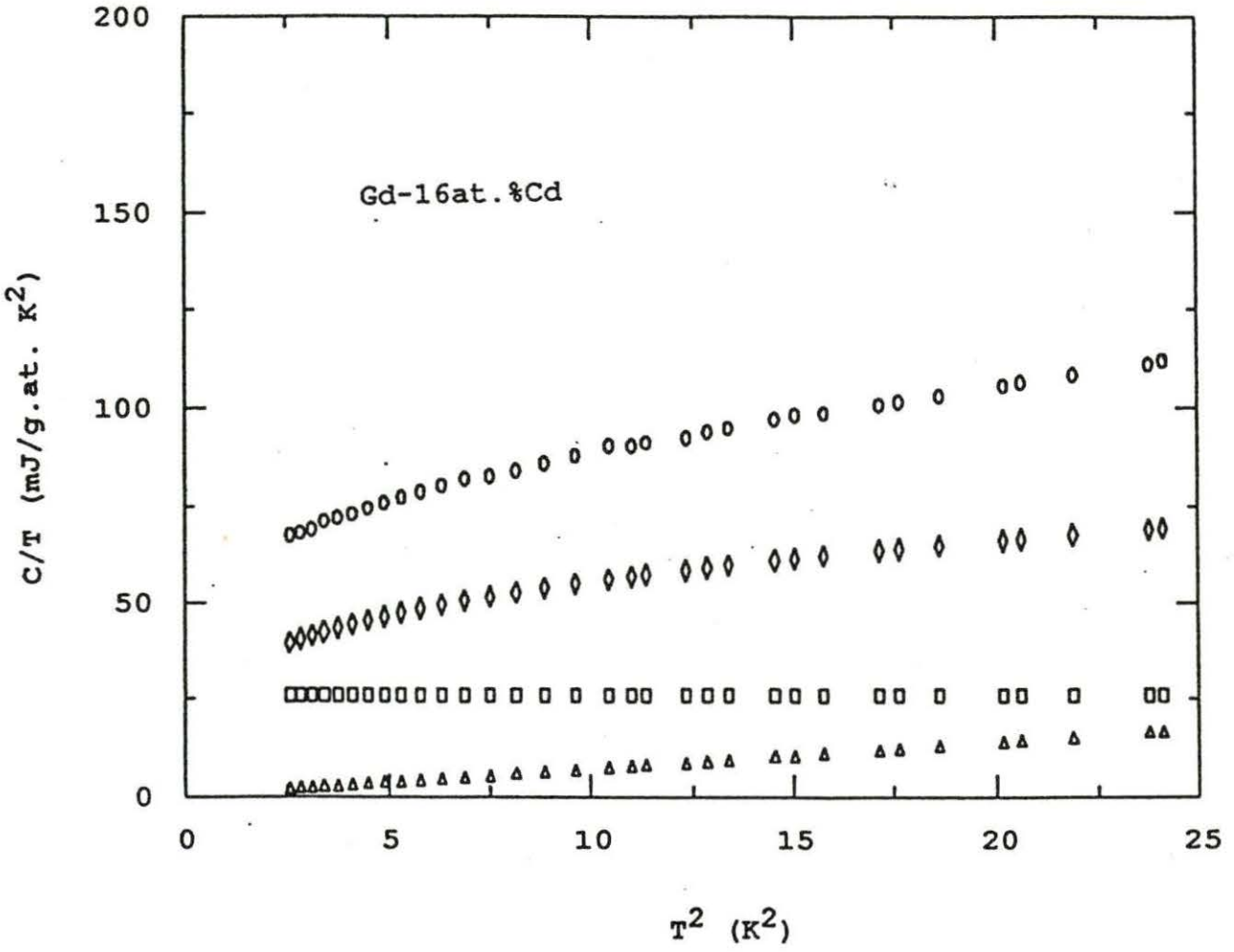

Fig. 15. C/T versus T^2 plot for lattice heat capacity (Δ), ferromagnetic (◊), sum of spin glass and electronic (□) and the total (○) heat capacities

C. Thermal Stability of Gd-Cd Alloys

The thermal stability of the metastable bcc Gd-Mg alloys has been studied by Herchenroeder and Gschneidner [6]. It was found that Gd-Mg alloys underwent a two-step reversion process on heating in which the bcc alloy first transformed into an intermediate metastable hcp phase at ~400 °C and then completely transformed to the equilibrium αGd + GdMg phases at 470 - 490 °C.

Similar experiments were carried out on Gd-Cd alloys. The differential thermal analysis (DTA) was made on all of the Gd-Cd samples using a Perkin-Elmer DTA unit. Samples of 30 - 150 mg were used, and the heating rate varied from 2 °C/min to 10 °C/min in order to obtain the optimum DTA data.

Shown in Fig. 16 is the DTA curve for sample Gd-17at.%Cd. It has two small peaks at 407 °C and 468 °C, respectively, indicating two exothermic reactions. A strong endothermic reaction can be seen at ~740 °C, corresponding to the eutectoid transformation from low temperature phase to high temperature

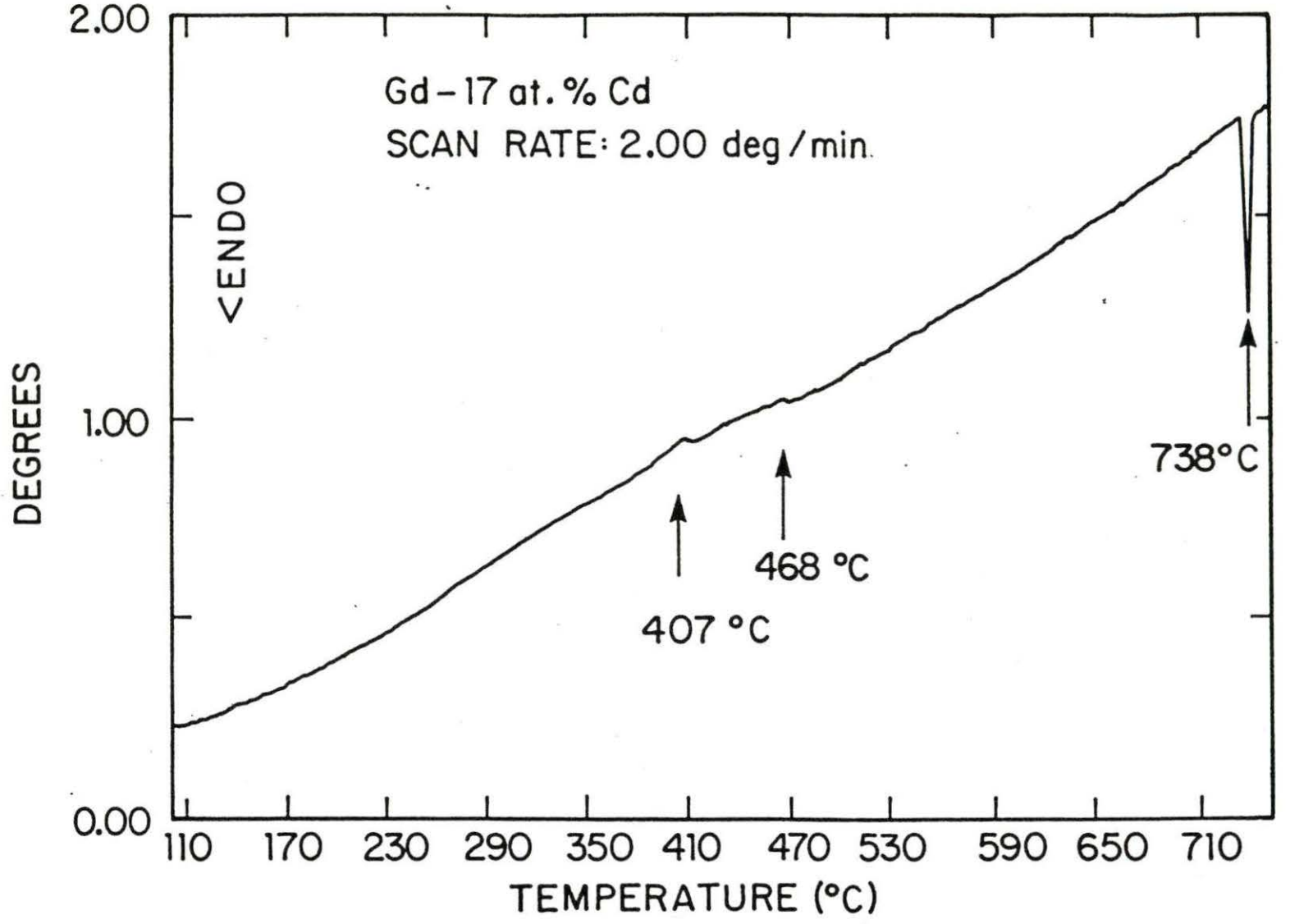

Fig. 16. Differential thermal analysis (DTA) curve for Gd-17at.%Cd

phase. The eutectoid temperature obtained from this study (738 °C) is slightly higher than the one reported earlier, 725°C, [9].

The two exothermic reactions in this system occur at about the same temperatures where the two reversion reactions take place in Gd-Mg system. It is, therefore, reasonable to say that bcc Gd-17at.%Cd undergoes a similar decomposition process as that of Gd-Mg alloys, i.e., bcc Gd-17at.%Cd first transforms to an intermediate hcp phase at 407 °C and then transforms to equilibrium αGd + CdGd phase at 468 °C. This two-step reversion reaction has been observed in all the Gd-Cd alloys as indicated in their DTA curves. For samples Gd-15at.%Cd and Gd-17at.%Cd, the two peaks in their DTA curves are clear, and the peak temperatures can be easily determined. For sample Gd-19at.%Cd, the lower peak occurs at a well defined temperature, but the upper peak is actually a broad maximum covering the temperature from 470 °C to 510 °C. In the case of Gd-16at.%Cd, both lower and upper peaks spread out over a quite wide temperature region. Figure 17 shows the reversion temperatures of the bcc Gd-Cd alloys as a function of Cd concentration. The uncertainties in the transformation temperatures as discussed above are indicated by the error bars, and for those points with no error bars, the

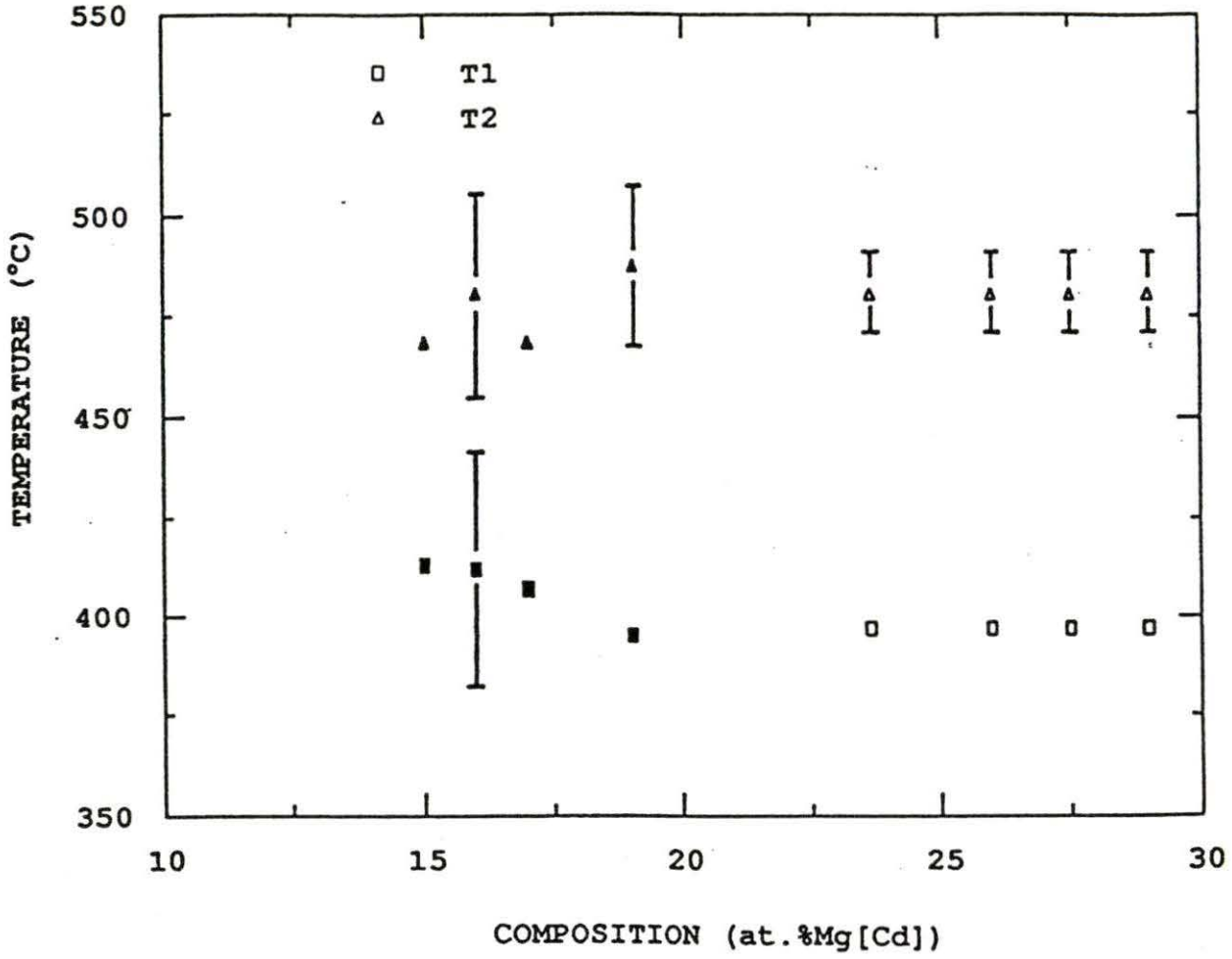

Fig. 17. The reversion temperatures of bcc Gd-Mg(Cd) alloys. Solid symbols are data from Gd-Cd system and open ones are from Gd-Mg system

uncertainties are about the same as the symbol size itself. T_1 increases as the Cd concentration moves towards eutectoid composition suggesting that bcc Gd-Cd alloys are more stable near the eutectoid composition. T_2 seems to be quite scattered and it is centered about 475 °C. The values of T_1 and T_2 are listed in Table 4. For comparison, the reversion temperatures of the bcc Gd-Mg alloys are also shown in Fig. 17.

The following experiments were carried out to determine the stability of bcc Gd-Cd alloys at lower temperatures. A piece of Gd-17at.%Cd sample was sealed in a quartz tube under He partial pressure and heated to 415 °C at a rate of 15 °C/min. The sample was quickly cooled to room temperature and X-ray examined. One would have expected that such a heat treated sample contain the intermediate hcp phase because it was heated just above T_1 (T_1 = 407 °C). The X-ray pattern showed, however, the existence of both hcp and CdGd peaks, indicating that CdGd phase has already precipitated out at this temperature. Another piece cut from the same sample was heated to 380 °C at a rate of 20 °C/min in a similar environment. X-ray examination showed again CdGd peaks in addition to the hcp αGd + bcc βGd pattern. This finding suggests that the second reversion reaction from the intermediate

Table 4. Reversion temperatures of bcc Gd-Cd alloys

Alloy	T_1 (°C)	T_2 (°C)
Gd-19at.%Cd	395 ± 2	487 ± 20
Gd-17at.%Cd	407 ± 2	468 ± 2
Gd-16at.%Cd	412 ± 30	480 ± 25
Gd-15at.%Cd	413 ± 2	468 ± 2

hcp phase to αGd + CdGd phase can start as early as ~380 °C, which is even below the first reversion temperature T_1.

The first reversion reaction took place far below T_1. It actually started at ~250 °C. This was indicated by the appearance of hcp peaks in the X-ray pattern of a sample which was heated to 250 °C under the similar condition. No peaks from CdGd could be identified. It seems to be the case that initial transformation from bcc Gd to the intermediate hcp phase starts quite early but releases very little energy possibly because only local atomic rearrangement are occurring. While the release of large amount of energy which could be detected by DTA occurs at a higher temperature T_1 as more atomic movement is possible. The situation is the same in the second reversion reaction from the intermediate hcp phase to the equilibrium αGd + CdGd phase.

The metastable bcc Gd phase was still evident in the X-ray pattern, after the sample was heated to 100, 250, 330 and 380 °C, respectively. Its absence was first noted in the sample heated to 415 °C, just above T_1. This is consistent with the above conclusion that the major portion of the transformation from bcc Gd to the intermediate hcp phase takes place near T_1.

III. CONCLUSION AND SUMMARY

As a continuation of the research on bcc Gd-Mg alloy system by Herchenroeder and Gschneidner, the metastable bcc Gd-Cd alloys were studied with the emphasis on their metallurgical and magnetic properties.

The bcc βGd was successfully retained at room temperature by alloying with Cd and subsequent ice water/acetone quenching from liquid phase. An essentially single phase alloy could be retained for Cd concentrations from 15 at.%Cd to 19 at.%Cd, which is in the vicinity of the eutectoid composition of βGd in the Gd-Cd system. The lattice constants obtained for these alloys were used to determine the lattice constant of pure bcc Gd by extrapolation to 0 at.%Cd. Good agreement between this extrapolated value and that obtained from Gd-Mg alloys by using the same method suggested the validity of such extrapolation method. Thermal stability of these metastable bcc Gd-Cd alloys was examined by using differential thermal analysis (DTA). Similar to Gd-Mg alloys, the Gd-Cd alloys underwent a two-step reversion process on heating in which the bcc alloy first

transformed into an intermediate distorted hcp phase and then transformed completely to the equilibrium αGd + CdGd phases. The initial transformation of the first reversion took place as early as 250 °C, which is at a lower temperature than that found in Gd-Mg system (300 °C). Consequently, the bcc phase is less stable in Gd-Cd system than in Gd-Mg system. This is not unexpected if one realizes the fact that the metallic radius of Gd is closer to that of Mg than to Cd. A relatively large size difference between Gd and Cd atoms makes bcc Gd-Cd alloys less stable.

The magnetic behavior of these Gd-Cd alloys is most interesting. They undergo a ferromagnetic phase transition at 77 - 88 K and then enter a spin glass + ferromagnetic mixed state at 23 - 36 K. This Gabay-Toulouse-type spin glass transition is clearly seen as one compares the susceptibilities of a sample cooled in zero field and in an applied field. That spin glass behavior exists over such a high Gd concentration (81 - 85 at.%Gd), which is by far the highest concentration of magnetic atom known to exhibit spin glass behavior in a crystalline metallic system, indicates the strong competition between ferromagnetic and antiferromagnetic interactions existing within the ferromagnetically ordered state. Low temperature heat

capacity can be deconvoluted into the lattice, ferromagnetic, spin glass and electronic contributions. The appearance of both ferromagnetic and spin glass heat capacity supports the conclusion that the final state is a mixed spin glass plus ferromagnetic state below T_f.

The ferromagnetic ordering temperature T_c was obtained for each alloy, and the T_c for pure bcc Gd was determined using an extrapolation method. T_c = 131 K is the result of combining the data from the Gd-Cd and Gd-Mg systems.

Knowing the values of T_c and T_f for Gd-Cd alloys, the magnetic phase diagram determined from Gd-Mg system can extended to high Gd concentration. Assuming that the magnetic property depends only on Gd concentration and is independent of the alloying elements, Cd or Mg, the high Gd concentration part is added to the magnetic phase diagram of Gd-Mg(Cd) and shown in Fig. 18. As Gd concentration increases, T_c increases and is approaching the Curie temperature of pure bcc Gd. On the contrary, T_f decreases with increasing Gd concentration and tends to become zero at a concentration ~ 90 at.%Gd.

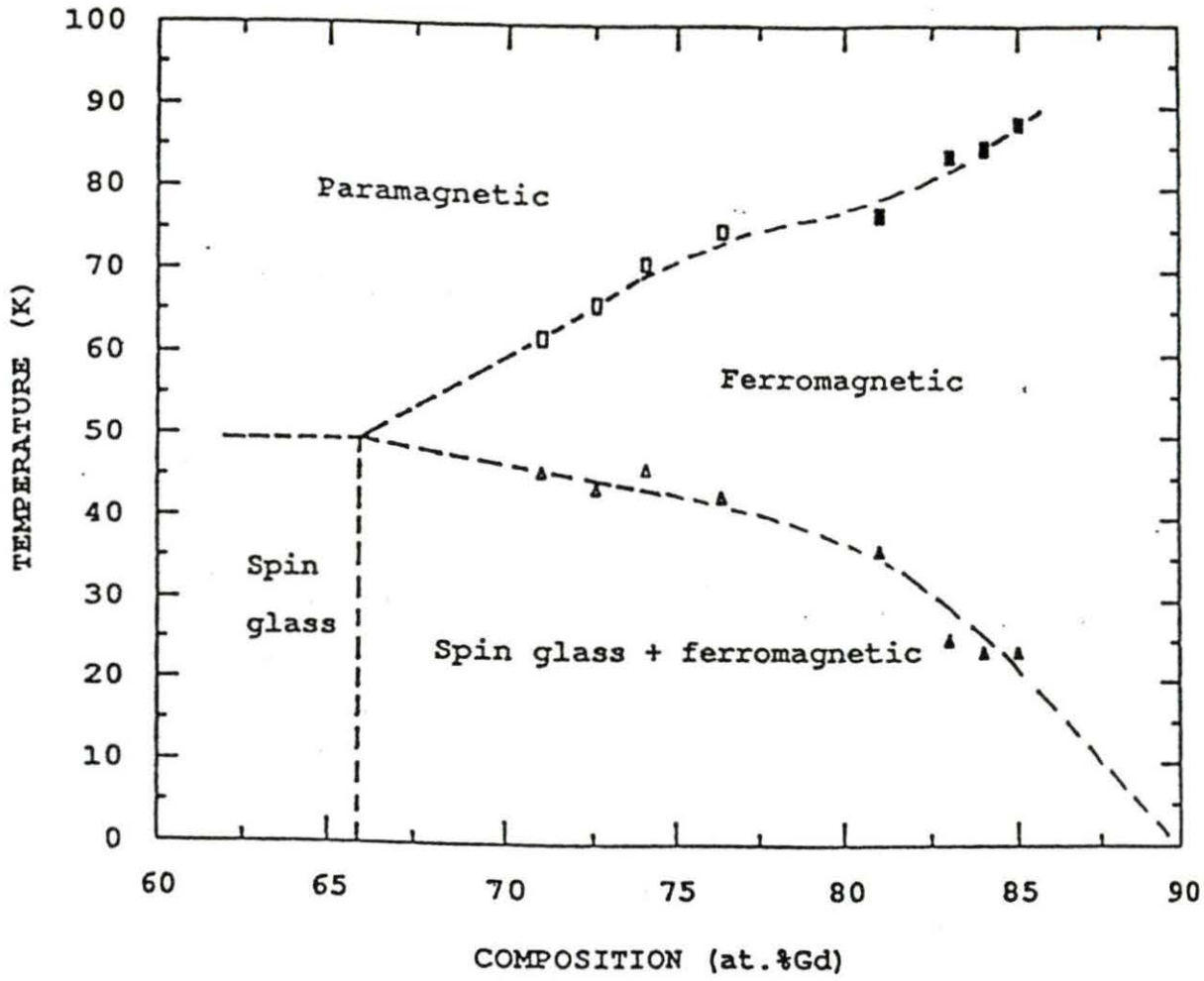

Fig. 18. Magnetic phase diagram of bcc Gd-Mg(Cd) alloy. Solid symbols are data from Gd-Cd system and open ones are from Gd-Mg system. □ : T_c; △ : T_f

IV. REFERENCES

[1] B. J. Beaudry and K. A. Gschneidner, Jr., Handbook on the Physics and Chemistry of Rare Earths ed. by K. A. Gschneidner, Jr. and L. Eyring (North-Holland Publishing Company, Amsterdam, 1978), vol. 1, p. 173; K. A. Gschneidner, Jr. and A. H. Daane, Handbook on the Physics and Chemistry of Rare Earths ed. by K. A. Gschneidner, Jr. and L. Eyring (Elsevier Science Publishers B.V., Amsterdam, 1988), vol. 11, p. 409.

[2] E. G. Gibson and O. N. Carlson, Trans. Am. Soc. Met., 52, 1084 (1960).

[3] A. E. Miller and A. H. Daane, Trans. Metall. Soc. AIME, 280, 568 (1964).

[4] J. W. Herchenroeder, P. Manfrinetti and K. A. Gschneidner, Jr., Physica, 135B, 445 (1985).

[5] J. W. Herchenroeder and K. A. Gschneidner, Jr., Bull. Alloy Phase Diag., 9, 2 (1988).

[6] J. W. Herchenroeder, P. Manfrinetti and K. A. Gschneidner, Jr., Metall. Trans. A, 20A, 1575 (1989).

[7] J. W. Herchenroeder and K. A. Gschneidner, Jr., Phys. Rev. B, 39, 11850 (1989).

[8] P. Manfrinetti and K. A. Gschneidner, Jr., J. Less-Common Metals, 123, 267 (1986).

[9] G. Bruzzone, M. L. Fornasini and F. Merlo, J. Less-Common Metals, 25, 295 (1971).

[10] R. J. Stierman, K. A. Gschneidner, Jr., T.-W. E. Tsang, F. A. Schmidt, P. Klavins, R. N. Shelton, J. Queen and S. Legvold, J. Magn. Magn. Mater., 36, 249 (1983).

[11] J. Tang, Ph.D. Thesis, Iowa State Univ. (1989).

[12] K. Ikeda, K. A. Gschneidner, Jr., B. J. Beaudry and U. Atzmony, Phys. Rev. B, 25, 4604 (1982).

[13] J. Crangle, The Magnetic Properties of Solids (Edward Arnold, London, 1977), p. 166.

[14] K. A. Gschneidner, Jr., CRC Handbook of Chemistry and Physics 69th ed., ed. by R. Weast (CRC Press, Boca Raton, FL, 1988), p. B-208.

[15] V. Cannella, J. A. Mydosh and J. I. Budnick, J. Appl. Phys., 42, 1689 (1971).

[16] K. Moorjani and J. M. D. Coey, Magnetic Glasses (Elsevier, Amsterdam, 1984).

[17] B. R. Coles, B. V. B. Sarkissian and R. H. Taylor, Phil. Mag., B37, 489 (1978).

[18] M. Gabay and G. Toulouse, Phys. Rev. Lett., 47, 201 (1981).

[19] R. D. Shull, H. Okamoto and P. A. Beck, Solid State Commun., 20, 863 (1976).

[20] H. Maletta, J. Appl. Phys., 53, 2185 (1982).

[21] J. Durand, Glassy Metals: Magnetic, Chemical and Structural Properties ed. by R. Hasegawa (CRC Press, Boca Raton, FL, 1983).

[22] G. T. Alfieri, E. Banks, K. Kanematsu and T. Ohoyama, J. Phys. Soci. of Japan, 23, 507 (1967).

[23] K. H. J. Buschow, J. Chem. Phys., 61, 4666 (1974).

[24] E. Gopal, Specific Heats at Low Temperatures (Plenum Press, New York, 1966).

[25] L. E. Wenger and P. H. Keesom, Phys. Rev. B, 13, 4053 (1976).

[26] L. R. Walker and R. E. Walstedt, Phys. Rev. Lett., 38, 514 (1977).

[27] T. C. Leung, X. W. Wang and B. N. Harmon, Physica B, 149, 131 (1988).

[28] N. W. Ashcroft and N. D. Mermin, Solid State Physics (Holt, Rinehart and Winston, New York, 1976), p. 461.

V. ACKNOWLEDGEMENTS

I would like to express my sincere thanks to my major professor Dr. Karl Gschneidner. Without his advice and understanding, the completion of this thesis would be impossible. More importantly, I have learned a great deal both from his enormously rich knowledge and his great personality during the time I worked with him.

I thank Jack Moorman for his help in maintaining the apparatuses and providing a trouble free environment.

I also thank Kevin Dennis, Qian Qiang, Hsu Chi-Ming and Chou Fangcheng for their assistance in analyzing the samples using SQUID magnetometers, SEM and DTA.

This work was performed at Ames Laboratory under contract No. W-7405-eng-82 with the U. S. Department of Energy. The United States government has assigned the DOE Report number IS-T 1474 to this thesis.